Journal of Mechanisms and Robotics. Received July 01, 2015;
Accepted manuscript posted October 16, 2015. doi:10.1115/1.4031808

An Extensible Continuum Robot with Integrated Origami Parallel Modules

Ketao Zhang
ASME Member
Centre for Robotics Research, King's College London, University of London
Strand, London WC2R 2LS, UK
ketao.zhang@kcl.ac.uk

Chen Qiu
ASME Student Member
Centre for Robotics Research, King's College London, University of London
Strand, London WC2R 2LS, UK
chen.qiu@kcl.ac.uk

Jian S Dai
ASME Fellow
Centre for Robotics Research, King's College London, University of London
Strand, London WC2R 2LS, UK
jian.dai@kcl.ac.uk

Abstract

This paper presents a novel design of extensible continuum robots in light of origami inspired folding techniques. The design starts from a modularized crease pattern, which consists of two triangular bases and three waterbomb bases, and generates the folding process for creating an origami parallel structure. The process further progresses to generate a compliant module with the origami parallel structure and a helical compression spring. A novel extensible continuum robot with the integrated compliant parallel modules is then proposed to imitate not only the bending motion but also the contraction of continuum apparatus in nature. Mapping the origami parallel structure to an equivalent kinematic model, the motion characteristics of the origami structure are unraveled in terms of kinematic principles. The analysis reveals the mixed rotational and translational motion of the origami parallel module and the virtual axis for yaw and pitch motion. Following the kinematics of the proposed continuum robot and features of the integrated helical

spring in each module, three actuation schemes and resultant typical working phases with a tendon driven system are presented. The design and analysis are then followed by a prototype of the extensible continuum robot with six integrated compliant modules connected in serial. The functionality of the proposed continuum robot with the origami parallel structure as its skeleton and the helical springs as the compliant backbone is validated by experimental results.

Keywords: Extensible Continuum Robot, origami, compliant module, parallel mechanism, kinematics

1 Introduction

The lightweight continuum robot without rigid links and identifiable kinematic joints enables biological analogous motion. The inherent compliance of this kind of robot distinguishes themselves from conventional discrete and serpentine robots that employ rigid links and commonly used kinematic pairs. Due to their inherent characteristics, continuum robots can be utilized as compliant manipulators, limbs of walking robots and positioning devices. With a wide range of potential applications, typical continuum robots have been developed in the last two decades. In terms of the method and location of mechanical actuation employed, continuum robots were broadly classified into three types including intrinsic, extrinsic and hybrid [1, 2].

Continuum and hyper-redundant robots allowing whole-arm manipulation of a wide range of objects with various shapes have been extensively investigated by the robotics research community. Wilson and Mahajan [3] presented a typical flexible manipulator with a series of polymeric tube elements and investigated their elastic deformation generated by internal fluid pressures. Chirikjian and Burdick [4] presented the design criteria of a 30-DOF planar

hyper-redundant manipulator and used it to validate a continuum approach to kinematics of this kind of robot. Sujan and Dubowsky [5] created an innovative lightweight hyper-redundant robot that consists of a serial chain of parallel stages and allows a compact configuration. Hannan and Walker [6, 7] explored the design of elephant's trunk robotic manipulator which was composed of 16 two-DOF joints and actuated by a cable servo system. With the presented design and the validated kinematic model of a continuum style robot, different strategies were implemented to demonstrate the capability of the robot for various tasks such as whole arm grasping. Subsequently, biologically inspired octopus-mimicking grasp-synergy functions were introduced to increase the usability of continuum manipulators and a framework for simplifying the creation of synergy-movements was developed [8]. Yoon and Yi [9] designed a 4-DOF flexible robot by connecting two continuum mechanisms and using springs as backbone for human-robot interaction tasks where safety is essential.

In addition to some study of continuum manipulators, continuum robots having the capability in rescue mission and hazardous areas are broadly developed to imitate locomotion of slim creatures. Most continuum robots for locomotion are snake-like robots, offering high stability and good terrainability [10]. With the biologically inspired robot termed Active Cord Mechanism (ACMIII) proposed by Hirose [11], bio-inspired robots including the snake-like robots have been widely investigated [12-14]. Analogously, Koh and Cho [15, 16] developed caterpillar-inspired biomimetic inchworm robot by employing origami-like structures and integrating shape-memory-allow (SMA) actuators. Using the recently developed robot fabrication method inspired by origami folding, Onal, Wood and Rus [17] presented a concept-case-study of a mobile robot that can implement worm-like peristaltic locomotion. Most recently, Zhang, Qiu and Dai [18] proposed a worm robot by integrating the kirigami parallel structure and SMA linear

actuators. Hoff, Jeong and Lee [19] proposed a thread-actuated origami robot for location and locomotion. In contrast to the locomotion of slim creatures, Godage, Nanayakkara and Galdwell [20] developed a quadruped-legged robot with continuum limbs and investigated the kinematic and dynamic modeling of the robot.

Further to the broad development of continuum robots for manipulation and locomotion, hyper-redundant and continuum robots have been developed for positioning applications particularly for scenarios with confined working space. Lim, et al. [21] developed an active catheter that could be used as surgical tools for minimally invasive diagnosis. Camarillo, et al. [22] investigated a planar single-section continuum manipulator as a single case of tendon-driven continuum manipulators and explored the underlying mechanics, mapping the desired beam configuration to tendon displacements. In recent years, a large number of new generations of steerable robots and hyper-redundant robots possessing high dexterity have been developed for positioning end-effectors and performing surgical tasks [23-28].

Origami-inspired technologies for "printable robotics" [29, 30] create an interesting trend in developing lightweight robots. Comparing to the traditional polymer-based soft robots [31], origami structures with compliant components are capable of imitating function of the skeleton of vertebrates. This allows origami folding based continuum robot providing certain stiffness to retain a desired body configuration.

Taking inherent properties of continuum robots and distinct characteristics of origami structures, this paper presents an approach for designing origami inspired extensible continuum robots by integrating origami structures as a skeleton and helical springs as a backbone. The design process of a 3-DOF origami parallel structure which is formed from a two-dimensional crease pattern drawn on a flat-sheet is introduced first. By integrating a helical spring into the

origami parallel structure, a compliant parallel module is created. This leads to a novel extensible continuum robot with six successively interfaced compliant modules in the case of this work. The virtual rotational axis and orientation of the upper platform of the compliant parallel module are explored in terms of geometry based kinematic principles. The kinematics of the continuum robot is then revealed in consideration of motion characteristics of the origami structure and features of the integrated helical spring in each module. A prototype of the robot with six modules actuated by three tendons is fabricated with paper made origami structure for the purpose of characteristic evaluation of the innovative design concept.

2 Design of an Origami Parallel Module and the Integrated Continuum Robot

An origami structure is formed by folding a single paper sheet with crease patterns in a variety of flexible ways. The underlying principles including geometric design [32-34] and mathematic modeling of origami folding interested artists and mathematicians. Recent interdisciplinary studies which bridge the art and engineering disciplines led to creative solutions in a variety of research areas such as mechanisms and robotics [35-40]. This section introduces the design process of a 3-DOF origami parallel structure and an integrated continuum robot with a tendon driven system.

2.1 The Origami Parallel Structure with Jointed Waterbomb Bases

The waterbomb crease base drawn on a piece of cardboard (or layered flat sheet material) in square shape is illustrated in Fig. 1(a), in which six creases are symmetrically distributed with respect to the axis passing points B_i and P_i. The crease base is also symmetrical with respect to two collinear creases that are perpendicular to axis B_iP_i. These creases have common point A_i, the centre of the square cardboard. All six panels are in isosceles right triangle shape with panels l_{i1}, l_{i2}

and l_{i6} are the mirror of panels l_{i3}, l_{i4} and l_{i5}, respectively. A crease pattern with three waterbomb bases, two equilateral triangular panels and two flaps is then formed by joining these crease bases in a 'Y' shape in Fig. 1(b).

Following the pre-grooved creases passing points B_1, B_2 and B_3 of the 2D crease pattern in Fig. 1(b), the flat cardboard is able to be folded to a half-erected configuration in Fig. 2(a). The cardboard is further folded by attaching two flaps to panels l_{14} and l_{34} and aligning two edges passing points P_1 and P_3 to creases joining flaps to triangular panel p. This leads to a three-dimensional closed-loop parallel structure [41]. A plane-symmetric 3D origami parallel structure is formed by folding the rest of creases and a schematic model of the origami parallel structure is illustrated in Fig. 2(b).

The origami parallel structure in Fig. 2(b) consists of a base b, a platform p, and three identical waterbomb bases that connect the platform to the base with creases. The parallel structure is symmetrical with respect to a virtual plane Π defined by common points A_1, A_2 and A_3 and the platform implements two rotations around axes located in the plane Π and one translation in the direction normal to the platform.

2.2 A Compliant Parallel Module Using the Origami Parallel Structure as Skeleton and a Spring as Backbone

A prototype of the origami parallel structure is obtained by folding 0.3 mm thick laminated sheets. In the presented model, each waterbomb crease base in 2D is a 20mm by 20mm square.

In order to avoid fatigue of creases induced by repetitive motion and strengthen the stiffness of the origami parallel structure, a steel helical compression spring (wire diameter 0.58 mm, external diameter 9.2 mm, spring height 15 mm and spring constant 0.59 N/mm) is used to provide

additional elasticity to the structure. The two distal ends of the spring are fixed to the base and platform of the parallel structure in Fig. 3. The compliance of the flexible creases is considered ignorable comparing to the compliance of the helical spring. This leads to a compliant module with the origami parallel structure determining the motion of the platform and the integrated spring characterizing the compliance of the module. When an external force is applied on the platform, it moves towards the base and the parallel structure changes to a compact configuration. In the opposite phase when the external constraint is released, the platform moves against the base resorting to elasticity of the embedded spring and the parallel structure will recover the contraction range.

2.3 An Evolved Extensible Continuum Robot

Taking the compliant parallel module as a module, a multi-section continuum mechanism is able to be formed by joining a number of compliant modules in serial. For each pair of adjacent compliant modules, the base of jth (j = 1, 2, …, n − 1) module is connected to the platform of the kth (k = 2, …, n) module by aligning creases and allowing the points P_{ij} and B_{ik} to be coincident. As shown in Fig. 4, six compliant parallel modules are integrated together following above procedure.

As the compliant module allows bending motion and contraction when applying asymmetrically and symmetrically distributed forces to the platform, a tendon driven actuation system is employed to achieve desired motion by routing three tendons via parallel paths passing guiding holes at corners of the triangular base and platform of each module. With three parallel tendons, one or two of the three tendons in tension lead to bending motion of the platform while all three tendons in tension lead to pure contraction or both bending motion and contraction. In the continuum robot, the bending motion and axial contraction of each module result in curved

bending motion and contraction of the multi-section robot.

3. The Virtual Rotation Axes and Orientation of the Platform of the Parallel Module

In the context of mechanisms [35, 36], kinematic mapping of the origami parallel structure is a parallel mechanism employs only 1-DOF revolute joints (R) and consists of two triangular bases and three closed-loop chain-legs, each of which is a spherical 6R linkage[41, 42]. The performance of the parallel origami structure is revealed by analyzing the kinematic equivalent in this section.

3.1 The Virtual Rotation Axis

To obtain the kinematic model of the equivalent parallel mechanism, the spherical 6R linkage in each chain-leg is taken as a spherical joint (S) with consideration of spherical motion of the 6R linkage and the equivalent serial limb is a RSR (R for revolute joint) kinematic chain. The common point A_i, the intersection of axes of six revolute joints of the 6R linkage, is the center of the equivalent spherical joint as illustrated in Fig. 5(a). Points B_i and B_i' are the vertices of base and platform of the equivalent parallel mechanism. Points C_i and C_i' are intersections of axes of revolute joints attached to the base and the platform, respectively.

To facilitate modeling, coordinate frames O_b-XYZ and O_p-uvw are attached to centres O_b and O_p of the base and the platform, respectively. As illustrated in Fig. 5(b), the parallel structure is in a general configuration and the platform and the base have a common line D_1D_2, where D_1 is the common point of axis C_1C_2 and its reflection $C_1'C_2'$, and D_2 is the common point of axis C_1C_3 and its reflection $C_1'C_3'$.

Since the triangular base and platform are symmetric with respect to plane Π, the w- and Z-axis are coplanar and have a common point F on the plane Π. The platform is rotating around a

virtual axis passing common point F. The virtual axis denoted by FG is perpendicular to the plane Π_1 defined by the w- and Z-axis. Further, plane Π_1 is the common normal plane of the platform and the base since these two axes are perpendicular to the platform and base, respectively. This reveals that common line D_1D_2 is perpendicular to plane Π_1 and parallel to virtual axis FG. It further derives that ED_2 is perpendicular to EO_p and EO_b simultaneously, where E denotes the common point of line D_1D_2 and the common normal plane Π_1 in Fig. 5(b).

Following the geometric analysis, unit vector $\mathbf{s}_\mathrm{e}$ in the direction of O_bE expressed in frame O_b $–XYZ$ is given by

$$\mathbf{s}_\mathrm{e} = \begin{bmatrix} \cos\delta \\ \sin\delta \\ 0 \end{bmatrix} \tag{1}$$

The unit vector $\mathbf{s}_\mathrm{en}$ parallel to common normal ED_2 is perpendicular to the vector $\mathbf{s}_\mathrm{e}$, it derives

$$\mathbf{s}_\mathrm{en} = \begin{bmatrix} \sin\delta \\ -\cos\delta \\ 0 \end{bmatrix} \tag{2}$$

The vector $\mathbf{r}_\mathrm{p}$, denoting the position of centre O_p in frame O_b $–XYZ$ is given by

$$\mathbf{r}_\mathrm{p} = r_0 \begin{bmatrix} \sin\psi\cos\delta \\ \sin\psi\sin\delta \\ \cos\psi \end{bmatrix} \tag{3}$$

where r_0 is the distance from centre O_p to centre O_b, angle ψ is measured from Z-axis to the vector $\mathbf{r}_\mathrm{p}$, the angle Φ ($\Phi = 2\psi$) and δ define yaw and pitch motion of the platform.

Considering the symmetric structure of the equivalent mechanism in Fig. 5, it obtains that $\mathbf{r}_\mathrm{p}$ is a normal vector of the symmetric plane. The common point M of line segment $O_\mathrm{b}O_\mathrm{p}$ and plane Π is the mid-point of $O_\mathrm{b}O_\mathrm{p}$. Given a vector $\mathbf{r}_\mathrm{nm}$ determining by point M and an arbitrary point N on the symmetric plane, vectors $\mathbf{r}_\mathrm{p}$ and $\mathbf{r}_\mathrm{nm}$ are perpendicular, meaning

$$\mathbf{r}_\mathrm{p} \cdot \mathbf{r}_\mathrm{nm} = 0 \tag{4}$$

where

$$\mathbf{r}_{nm} = \mathbf{r}_m - \mathbf{r}_n = \frac{r_0}{2}\begin{bmatrix}\sin\psi\cos\delta\\ \sin\psi\sin\delta\\ \cos\psi\end{bmatrix} - \begin{bmatrix}x\\ y\\ z\end{bmatrix}$$

Since point F is the common point of Z-axis and plane Π, the position vector of point F can be derived by substituting $x = 0$ and $y = 0$ into Eq. (4), that is

$$\mathbf{r}_f = \begin{bmatrix}0\\ 0\\ r_0^2/2\cos\psi\end{bmatrix} \tag{5}$$

Hence, the virtual rotation axis of the platform expressed in the frame O_b –XYZ is derived as

$$\mathbf{S}_v = \begin{bmatrix}\mathbf{s}_e\\ \mathbf{r}_f \times \mathbf{s}_e\end{bmatrix} \tag{6}$$

3.2 Orientation of the Upper Platform

Since the base and platform are symmetric with respect to plane Π, position and orientation parameters r_0, ψ and δ of the platform are uniquely defined by a set of l_i(i = 1, 2 and 3), where l_i is measured between vertex C_i of the base and C_i' of the platform.

The position vector of vertices C_i of the triangular base expressed in global frame O_b-XYZ are given by

$$\mathbf{c}_i = \begin{bmatrix}2r\cos(\phi_i + \pi/3)\\ 2r\sin(\phi_i + \pi/3)\\ 0\end{bmatrix} \tag{7}$$

Considering the symmetry of the vertices C_i and C_i' with respect to the plane Π, vector $\mathbf{l}_i$ pointing from point C_i to point C_i' is parallel to normal vector $\mathbf{n}$ and the distances between points C_i and C_i' are given by

$$\mathbf{L} = 2\mathbf{C}^T \cdot \mathbf{n} - r_0\mathbf{I} \tag{8}$$

where $\mathbf{I}$ is the identity matrix,

$$\mathbf{L} = \begin{bmatrix}l_1\\ l_2\\ l_3\end{bmatrix},\quad \mathbf{C} = \begin{bmatrix}c_1 & c_2 & c_3\end{bmatrix}^T \text{ and } \mathbf{n} = \begin{bmatrix}\sin\psi\cos\delta\\ \sin\psi\sin\delta\\ \cos\psi\end{bmatrix}.$$

Given a set of inputs l_i(i = 1, 2 and 3), the normal vector **n** is uniquely defined by Eq. (8). It implies that the orientation of the platform is determined by between points C_i and C_i'.

The angles δ and ψ are the parameters representing the orientation of the platform and can be yielded from Eq. (8), which are

$$\delta = \arccos(\pm \frac{l_1 - 2l_2 + l_3}{2\sqrt{l_1^2 + l_2^2 + l_3^2 - l_1 l_2 - l_2 l_3 - l_1 l_3}}) \tag{9}$$

$$\psi = \arccos(\pm \frac{2\sqrt{l_1^2 + l_2^2 + l_3^2 - l_1 l_2 - l_2 l_3 - l_1 l_3}}{6r}) \tag{10}$$

It further reveals that bending angle θ of the parallel module is also uniquely defined and given by

$$\theta = 2\psi \tag{11}$$

The proposed origami parallel module has the advantage of providing a bending motion with maximum range up to 45º and a squeezing degree of freedom that enables axial displacement.

With symmetric structure of the parallel module and its kinematics equations in Eqs. (7) and (8), the position and orientation of the platform are determined by the distance between each pair of points C_i and C_i'. This implies kinematics of each module of the presented multi-section continuum robot purely depends on the origami parallel structure but the central spring. This property distinguish the proposed design of the continuum robot with respect to other developments where the bending motion relies on elastic deformation of materials and the kinematics and mechanics are strongly coupled.

4. Kinematic Analysis and Workspace of the Continuum Robot with Integrated Compliant Modules

The origami parallel structure allows the continuum robot to implement both bending motion

and contracting motion. In this section, kinematics and workspace of the continuum robot are explored.

Since there is a virtual axis of rotation of each origami parallel module and the analytical form of the expression of rotation axis is derived, the kinematic model of the continuum robot can be modeled with the D-H method.

To facilitate the deriving of the kinematics, the reference frame for each module is assigned respectively from the base to the distal end of the robot in Fig. 6. The frames attached at the fixed base and distal end of the continuum robot are O_b-XYZ and O_d-$x_d y_d z_d$, respectively. The jth coordinate frame O_j-$x_j y_j z_j$ (j = 2, 3, …, 6) are attached to the platform of the ith ($i = j - 1$) module. As illustrated in Fig. 6, all the virtual axes of six modules are parallel to each other and perpendicular to the common normal plane defined by the z_i axes.

The forward kinematics of the continuum robot is to derive both position and orientation of the distal end of the robot. In a curved bending configuration of the continuum robot, points F_i in the normal plane is evenly distributed on a circular arc in Fig. 6 since all six modules have same origami structure and identical helical springs.

The continuum robot is in its home configuration when the tendons do not exert tensile forces and the z_i axes are collinear with the Z_b-axis. The guiding holes for tendons are located at points C_i and C_i'. The lengths of all three tendons in the home configuration are equal and denoted by L_0, which is also the original length of the robot. The robot generates symmetric flexion and extension when tendons are wound and released by rotating the pulleys independently. When the effective length of each tendon reduces to L_i ($L_i < L_0$), the distance between each pair of points C_i and C_i' is derived as

$$l_i = \frac{L_i}{n} \tag{12}$$

in which n is the number of integrated parallel modules and $n = 6$ in the present robot.

Substituting Eq. (12) into Eq. (8), the parameters ψ and δ which define yaw and pitch angle and the position vector $\mathbf{r}_p$ of the platform of each module can be calculated. Subsequently, the position vector of the continuum robot is derived as

$$\mathbf{r}_d = {}^{b}\mathbf{T}_2\,{}^{2}\mathbf{T}_3\,{}^{3}\mathbf{T}_4\,{}^{4}\mathbf{T}_5\,{}^{5}\mathbf{T}_6\,{}^{6}\mathbf{T}_d\mathbf{r}_p \tag{13}$$

in which

$${}^{b}\mathbf{T}_2 = \mathbf{R}(\delta)\mathbf{R}(\psi)\mathbf{P}(r_0)\mathbf{R}(\psi) \quad \text{and} \quad {}^{2}\mathbf{T}_3 = {}^{3}\mathbf{T}_4 = {}^{4}\mathbf{T}_5 = {}^{5}\mathbf{T}_6 = {}^{6}\mathbf{T}_d = \mathbf{R}(\psi)\mathbf{P}(r_0)\mathbf{R}(\psi)$$

The orientation of the robot is determined by the yaw and pitch angles δ and ψ of each module.

Reachable workspace of the continuum robot with respect to the global coordinate frame is reported in Fig. 7, where the Figs. 7(a) and 7(b) illustrate view of the workspace along Z-axis and Y-axis. The solid portion in the center of each view in Fig.7 represents the workspace of first parallel module attached to base. It shows workspace of this continuum robot is expanded with six modules connected in serial.

The inverse kinematics of the continuum robot is to derive the expected actuation range of tendons for a given position and orientation of the distal end.

Given the parameters ψ_d, δ and r_d of the distal end, r_0 can be derived by using the transformation matrix in Eq. (13) and $\psi = \psi_d/2n$. Hence, the expected input l_i of the tendons can be derived by substituting the parameter ψ, δ and r_0 into Eq. (8).

5. Characteristic Evaluation of the Continuum Robot in Three types of Actuation Schemes

Both bending motion and contracting motion of the continuum robot with six identical modules were evaluated in experimental tests. In this section, the experiment results for concept

evaluation are reported.

For a compression spring within its elastic limit, the applied force and the pure axial displacement obey Hooke's law, meaning the force is linearly proportional to the displacement. However, there is no analytical formula for the performance of the bending motion of normal compression springs. The bending performance of the integrated helical compression spring, where the external force is not aligned to the central axis, was verified with tests and the results in Fig.8 show the force is no longer proportional to the displacement of tendon guiding point in Fig. 8(a).

Since each origami module is a 3-DOF parallel mechanism capable of mixed motion including two rotations and one translation, the compliant module with embedded steel spring has two typical working phases including the bending motion and axial contracting motion. These two phases are enabled by three types of actuation schemes of the tendons, which are

(a) bending motion driven by tensile force exerted by only one tendon in tension;

(b) bending motion driven by tensile forces exerted by two tendons in tension;

(c) pure contraction driven by tensile forces exerted by three tendons in tension.

A list of actuation models for the above working phases using three tendons routing through parallel paths via tendon guiding points are enumerated in Table 1.

With consideration of both working phases of one individual compliant module and the kinematic modeling of the integrated continuum robot with successively interfaced modules, an experiment setup was constructed with a linear guide and a 6-DOF ATI nano17 force-torque sensor mounted on a moving stage. A prototype of the continuum robot was mounted on the fixed stage of the linear guide with the base of the robot perpendicular to the axial direction of the linear guide.

As listed in Table 1, each module has three types of actuation schemes. Accordingly, the

performance of the integrated continuum robot is evaluated following the three types of actuation schemes of the tendon driven system.

The first set of tests was conducted when the continuum robot is driven by only one tendon which provides a tensile force to the distal end of the robot. The experiment shows that one tensile force leads to bending motion in a normal plane defined by the path of the tendon in tension and the maximum bending angle of the distal end is larger than 180º as illustrated in Fig. 9 where Δl_1 is displacement representing the reduced length of the tendon.

The second set of tests was conducted when the continuum robot is driven by two tendons which provide two tensile forces. The experiments show that two tensile forces also leads to bending motion in the normal plane defined by the path of the tendon not in tension as illustrated in Fig. 10. The maximum bending angle of the distal end is smaller than the range of single tendon mode.

The third set of tests was conducted when the continuum robot is driven by all three tendons providing three tensile forces. These tests are more general cases where both contraction and bending motion are generated, while the pure contraction is shown in Fig. 11.

The preliminary experiment results prove the conceptual design of this novel continuum robot which possesses not only bending motion but also mixed contracting and bending motion. The distinct motion characteristics of the robot allow a range of application cases such as whole arm manipulation and snake-and worm-robot for locomotion.

Since the integrated helical spring in each compliant module is a traditional compression spring, the statics based modelling of the bending performance of the robot has to be further revealed.

6. Conclusions

This paper proposed a novel extensible continuum robot by integrating origami-inspired compliant modules. The study firstly presented the design process of a 3-DOF origami parallel structure folded from a two-dimensional crease pattern on a flat-sheet material. By integrating a helical spring as a backbone and the origami parallel structure as skeleton, a compliant parallel module was formed. Taking the compliant module as a segmental unit, a continuum robot with successively connected compliant modules and its tendon driven system were presented. The virtual rotation axis and its induced orientation of the upper platform in the origami parallel module were explored in terms of the kinematic principle. The analysis proved that kinematics of the origami parallel structure is decoupled from the spring mechanics. The kinematics of the robot was further derived in accordance with motion characteristics of each origami parallel module and with the integrated hybrid structure of the continuum robot. A prototype of the continuum robot with six integrated parallel modules was fabricated. Experimental results demonstrated two typical working phases including axial contraction and elongation, and bending motion of the presented design for the extensible continuum robot. The large bending angle and extensibility shown in the tests proved the functionality of the lightweight continuum robot.

Comparing to the traditional design of the continuum robots, the proposed design of the continuum robot based on origami folding technologies provided an interesting approach for developing robotic systems inspired by continuum creatures in nature.

Acknowledgments

The authors thank the European Commission for the support in the human-robot interaction project SQUIRREL in the name of Clearing Clutter Bit by Bit under grant number 610532 and the support of the National Natural Science Foundation of China under grant No.51205016.

References

[1] Robinson, G., and Davies, J. B. C., 1999, "Continuum robots-a state of the art." *Proceedings 1999 IEEE International Conference on Robotics and Automation*, **4**, pp. 2849-2854.

[2] Webster, R. J., and Jones, B. A., 2010, "Design and kinematic modeling of constant curvature continuum robots: A review." *The International Journal of Robotics Research*, **29**(13), pp. 1661-1683.

[3] Wilson, J. F., and Mahajan, U., 1989, "The mechanics and positioning of highly flexible manipulator limbs." *ASME J. Mech. Des.*, **111**(2), pp. 232-237.

[4] Chirikjian, G. S., and Burdick, J. W., 1994, "A hyper-redundant manipulator." *IEEE Robotics and Automation Magazine*, **1**(4), pp. 22-29.

[5] Sujan, V. A., and Dubowsky, S., 2004, "Design of a lightweight hyper-redundant deployable binary manipulator." *ASME J. Mech. Des.*, **126**(1), pp. 29-39.

[6] Hannan, M. W., and Walker, I. D., 2000, "Analysis and initial experiments for a novel elephant's trunk robot." *Proceedings of 2000 IEEE/RSJ International Conference on Intelligent Robots and Systems*, **1**, pp. 330-337.

[7] Hannan, M. W., and Walker, I. D., 2003, "Kinematics and the implementation of an elephant's trunk manipulator and other continuum style robots." *Journal of Robotic Systems*, **20**(2), pp. 45-63.

[8] William, M., and Walker, I. D., 2008, "Octopus-inspired grasp-synergies for continuum manipulators." *2008* IEEE *International Conference on Robotics and Biomimetics*, pp. 945-950

[9] Yoon, H. S., and Yi, B. J., 2009, "A 4-DOF flexible continuum robot using a spring backbone." *IEEE 2009 International Conference on Mechatronics and Automation*, pp. 1249-1254.

[10] Transeth, A. A., Pettersen, K. Y., and Liljebäck, P., 2009, "A survey on snake robot modeling and locomotion." *Robotica*, **27**(07), pp. 999-1015.

[11] Hirose, S., 1993 *Biologically Inspired Robots: Snake-Like Locomotors and Manipulators*. Oxford University Press, Oxford.

[12] Klaassen, B., and Paap, K. L., 1999, "GMD-SNAKE2: a snake-like robot driven by wheels and a method for motion control." *Proceedings of 1999 IEEE International Conference on Robotics and Automation*, **4**, pp. 3014-3019

[13] Nilsson, M., 1997, "Snake robot free climbing." *In 1997 IEEE International Conference on Robotics and Automation*, **4**, pp. 3415-3420.

[14] Wright, C., Johnson, A., Peck, A., McCord, Z., Naaktgeboren, A., Gianfortoni, P., and Choset, H., 2007, , "Design of a modular snake robot." *In 2007 IEEE/RSJ International Conference on Intelligent Robots and* Systems, pp. 2609-2614.

[15] Koh, J., Cho, K., 2010, "Omegabot: Crawling robot inspired by Ascotis Selenaria", *2010 IEEE International Conference on Robotics and Automation (ICRA)*, pp.109-114.

[16] Koh, J., Cho, K., 2013, "Omega-Shaped Inchworm-Inspired Crawling Robot with Large-Index-and-Pitch (LIP) SMA Spring Actuators", *IEEE/ASME Transactions on Mechatronics*, **18**(2), pp.419-429.

[17] Onal, C.D., Wood, R.J., Rus, D., 2013, "An Origami-Inspired Approach to Worm Robots", *IEEE/ASME Transactions on Mechatronics*, **18(**2), pp.430-438.

[18] Zhang, K., Qiu, C., and Dai, J. S., 2015, "Helical Kirigami-Enabled Centimeter-Scale Worm Robot with Shape-Memory-Alloy Linear Actuators." *ASME J. Mech. Rob.*, **7**(2), p.021014.

[19] Vander Hoff, E., Jeong, D., and Lee, K. 2014, "OrigamiBot-I: A thread-actuated origami robot for manipulation and locomotion." *In 2014 IEEE/RSJ International Conference on Intelligent Robots and Systems*, pp. 1421-1426.

[20] Godage, I. S., Nanayakkara, T., and Caldwell, D. G., 2012, "Locomotion with Continuum Limbs." *IEEE/RSJ International Conference on Intelligent Robots and Systems*, pp. 293-298.

[21] Lim, G., Minami, K., Yamamoto, K., Sugihara, M., Uchiyama, M., and Esashi, M., 1996, "Multi-link active catheter snake-like motion." *Robotica*, **14**(05), pp. 499-506.

[22] Camarillo, D. B., Milne, C. F., Carlson, C. R., Zinn, M. R., and Salisbury, J. K., 2008, "Mechanics modeling of tendon-driven continuum manipulators." *IEEE Transactions on Robotics*, **24**(6), pp. 1262-1273.

[23] Ota, T., Degani, A., Schwartzman, D., Zubiate, B., McGarvey, J., Choset, H., and Zenati, M. A., 2009, "A highly articulated robotic surgical system for minimally invasive surgery." *Ann. Thoracic Surgery*, **87**, pp. 1253-1256.

[24] Shang, J., Payne, C. J., Clark, J., Noonan, D. P., Kwok, K. W., Darzi, A., and Yang, G. Z., 2012, "Design of a multitasking robotic platform with flexible arms and articulated head for minimally invasive surgery." *In 2012 IEEE/RSJ International Conference on Intelligent Robots and Systems*, pp. 1988-1993.

[25] Tognarelli, S., Salerno, M., Tortora, G., Quaglia, C., Dario, P., and Menciassi, A., 2012, "An endoluminal robotic platform for Minimally Invasive Surgery." *In 2012 4th IEEE RAS & EMBS International Conference on Biomedical Robotics and Biomechatronics (BioRob)*, pp. 7-12.

[26] Vitiello, V., Lee, S. L., Cundy, T. P., and Yang, G. Z. 2013, "Emerging robotic platforms for minimally invasive surgery." *IEEE Reviews in Biomedical Engineering*, 6, pp. 111-126.

[27] Qi, P., Qiu, C., Liu, H., Dai, J. S., Seneviratne, L., Althoefer, K., 2014, "A Novel Continuum-Style Robot with Multilayer Compliant Modules," *2014 IEEE/RSJ International Conference on Intelligent Robots and Systems*, Chicago, IL, Sept., pp. 3175-3180.

[28] Qi, P., Liu, H., Seneviratne, L., Althoefer, K., 2014, "Towards Kinematic Modeling of a Multi-DOF Tendon Driven Robotic Catheter," *36th Annual International Conference of the IEEE Engineering in Medicine and Biology Society (EMBC)*, Chicago, IL, Aug., pp. 3009-3012.

[29] Onal, C. D., Wood, R. J., Rus, D., 2011, "Towards printable robotics: Origami-inspired planar fabrication of three-dimensional mechanisms." *2011 IEEE International Conference on Robotics and Automation (ICRA)*, May, pp. 4608-4613.

[30] Gafford, J.B., Kesner, S.B., Wood, R.J., Walsh, C.J., 2013, "Force-sensing surgical grasper enabled by pop-up book MEMS," *2013 IEEE/RSJ International Conference on Intelligent Robots and Systems (IROS),* Nov. pp.2552-2558,

[31] Rus, D., Tolley, M. T., 2015, "Design, fabrication and control of soft robots." *Nature*, **521**(7553), pp.467-475.

[32] Lang, R. J., 2011, *Origami design secrets: mathematical methods for an ancient art*. CRC Press, NW.

[33] Hoffmann, R., 2001, "Airbag Folding: Origami Design applied to an Engineering Problem", *Proc. of the 3rd Int. Meeting of Origami Science, Math, and Education*, March 9-11, Asilomar, CA, USA.

[34] Miura, K., 1989, "A Note on Intrinsic Geometry of Origami". *In Research of Pattern Formation*, KTK Scientific Publishers, pp. 91-102.

[35] Dai, J. S., and Rees Jones, J., 2002, "Kinematics and mobility analysis of Origami carton folds in packing manipulation based on the mechanism equivalent," *Journal of Mechanical Engineering Science, Proc. IMechE,* **216**(10), pp. 959-970.

[36] Dai, J. S., and Rees Jones, J., 1999, "Mobility in Metamorphic Mechanisms of Foldable/Erectable Kinds," *ASME J. Mech. Des.*, **121**(3), pp. 375–382.

[37] Rodriguez-Leal, E., and Dai, J. S., 2007, "From Origami to a New Class of Centralized 3-DOF Parallel Mechanisms", *Proceedings of the ASME 2007 International Design Engineering Technical Conferences & Computers and Information in Engineering Conference*, Las Vegas, Nevada, USA, DETC2007-35516.

[38] Winder, B. G., Magleby, S. P., Howell, L. L., 2009, "Kinematic representations of pop-up paper mechanisms". *ASME J. Mech. Rob.*, **1**(2), p. 021009.

[39] Bowen, L. A., Grames, C. L., Magleby, S. P., Lang, R. J., and Howell, L. L., 2013, "An Approach for Understanding Action Origami as Kinematic Mechanisms", *ASME 2013 International Design Engineering* Technical *Conferences and Computers and Information in Engineering Conference*, DETC2013-13407.

[40] Abdul-Sater, K., Winkler, M.M., Irlinger, F., Lueth, T.C., 2015, "Three-Position Synthesis of Origami-Evolved, Spherically Constrained Spatial Revolute–Revolute Chains." *ASME J. Mech. Rob.*, **8**(1), p.011012.

[41] Zhang, K., Fang, Y., Fang, H., Dai, J. S., 2010, "Geometry and Constraint Analysis of the 3-Spherical Kinematic Chain Based Parallel Mechanism". *ASME J. Mech. Rob.*, **2**(3), p. 031014.

[42] Salerno, M., Zhang, K., Menciassi, A. and Dai, J. S., 2014, "A Novel 4-DOFs Origami Enabled, SMA Actuated, Robotic End-effector for Minimally Invasive Surgery". *2014 IEEE International Conference on Robotics and Automation (ICRA2014)*, Hong Kong, No. 1137

List of table captions

Table 1. Working phases of the compliant module

Journal of Mechanisms and Robotics. Received July 01, 2015;
Accepted manuscript posted October 16, 2015. doi:10.1115/1.4031808

Table 1 Working phases of the compliant module

Working phases	Tensile force(s)	Length of tendons		
		l_1	l_2	l_3
Bending motion	One tendon in tension	$< L_0$	$> L_0$	$> L_0$
		$< L_0$	$< L_0$	$> L_0$
		$< L_0$	$> L_0$	$< L_0$
	Two tendons in tension	$> L_0$	$> L_0$	$< L_0$
		$> L_0$	$< L_0$	$< L_0$
		$> L_0$	$< L_0$	$> L_0$
Pure contraction	Three tendons in tension	$l_1 = l_2 = l_3$		

List of figure captions

Fig. 1. A 2D crease pattern with three waterbomb bases (a) 2D waterbomb crease base (b) a crease pattern with bilateral symmetry

Fig. 2. Schematic model of two stages in the folding process of the origami structure: (a) a half-erected configuration, (b) the completed origami parallel structure

Fig. 3. Components of the compliant module: (a) a paper made origami-parallel structure, (b) helical spring connecting the base and platform

Fig. 4. A prototype of the proposed extensible continuum robot with six parallel modules

Fig. 5. Kinematic model of the equivalent mechanism of the origami parallel structure

Fig. 6. Schematic kinematic model of the continuum robot with six modules

Fig. 7. Workspace of the continuum robot (a) view along Z-axis (b) view along Y-axis

Fig. 8. Verification of the nonlinear performance of the compression spring (a) test set-up (b) bending performance of the compression spring

Fig. 9 Sequential stop figures of bending motion generated by one tensile force

Fig. 10. Sequential stop figures of bending motion generated by two tensile forces

Fig. 11. The compact and elongated configurations of the extensible continuum robot

Journal of Mechanisms and Robotics. Received July 01, 2015;
Accepted manuscript posted October 16, 2015. doi:10.1115/1.4031808

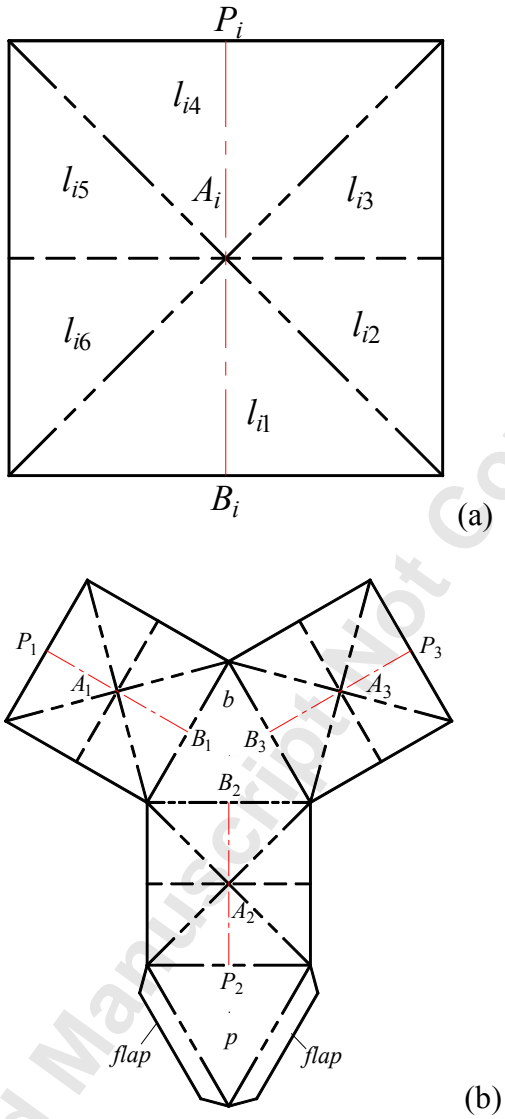

Fig. 1. A 2D crease pattern with three waterbomb bases (a) 2D waterbomb crease base (b) a crease pattern with bilateral symmetry

Journal of Mechanisms and Robotics. Received July 01, 2015;
Accepted manuscript posted October 16, 2015. doi:10.1115/1.4031808

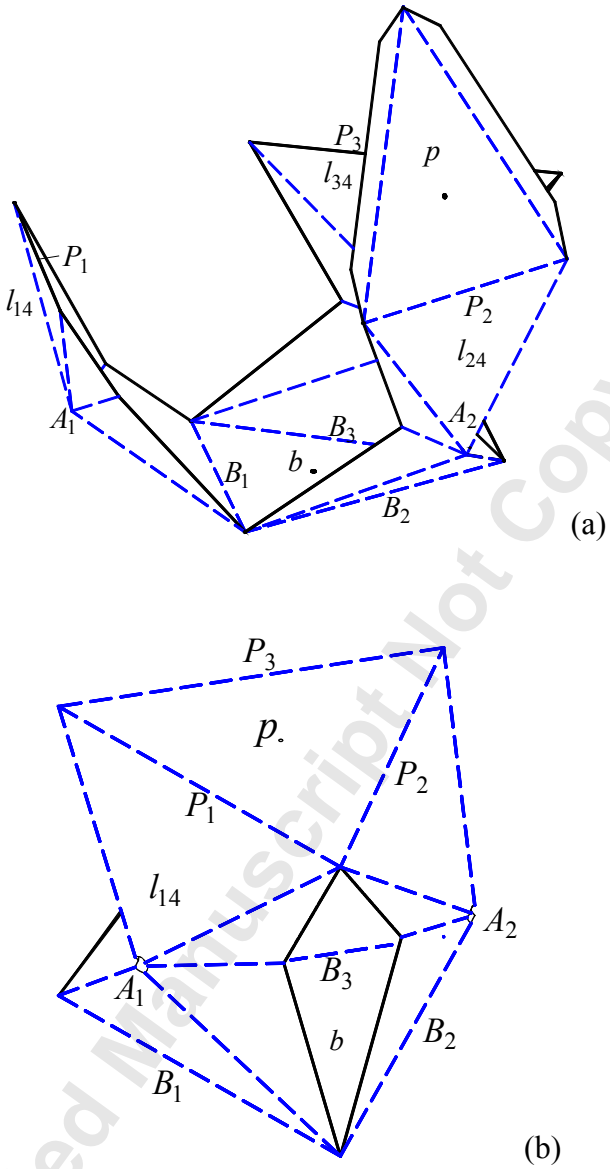

Fig. 2. Schematic model of two stages in the folding process of the origami structure: (a) a half-erected configuration, (b) the completed origami parallel structure

Journal of Mechanisms and Robotics. Received July 01, 2015;
Accepted manuscript posted October 16, 2015. doi:10.1115/1.4031808

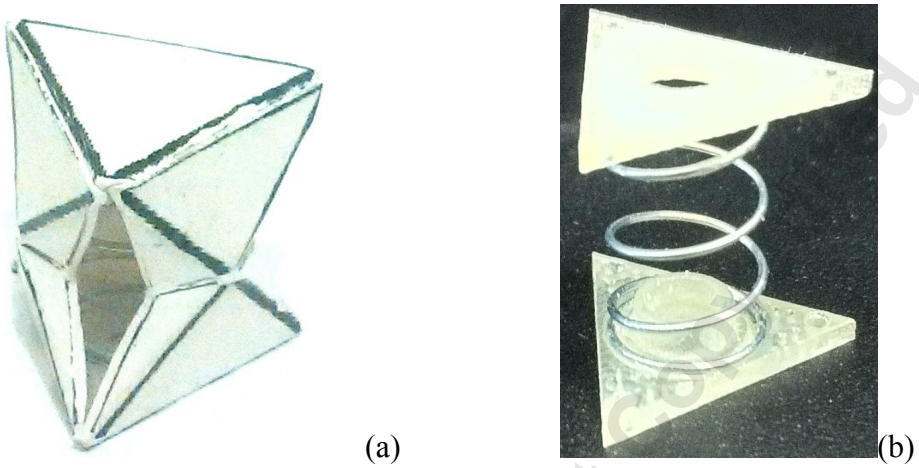

(a) (b)

Fig. 3. Components of the compliant module: (a) a paper made origami-parallel structure, (b) helical spring connecting the base and platform

Journal of Mechanisms and Robotics. Received July 01, 2015;
Accepted manuscript posted October 16, 2015. doi:10.1115/1.4031808

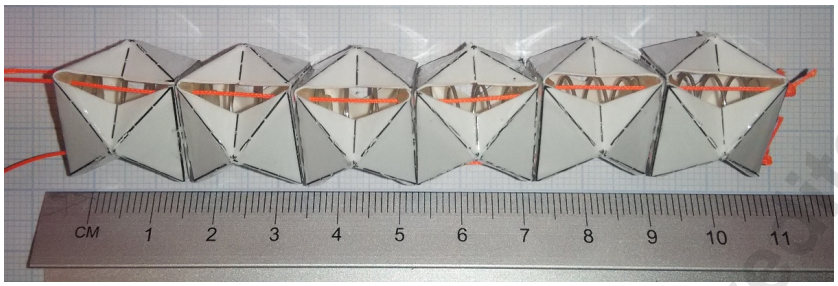

Fig. 4. A prototype of the proposed extensible continuum robot with six parallel modules

Journal of Mechanisms and Robotics. Received July 01, 2015;
Accepted manuscript posted October 16, 2015. doi:10.1115/1.4031808

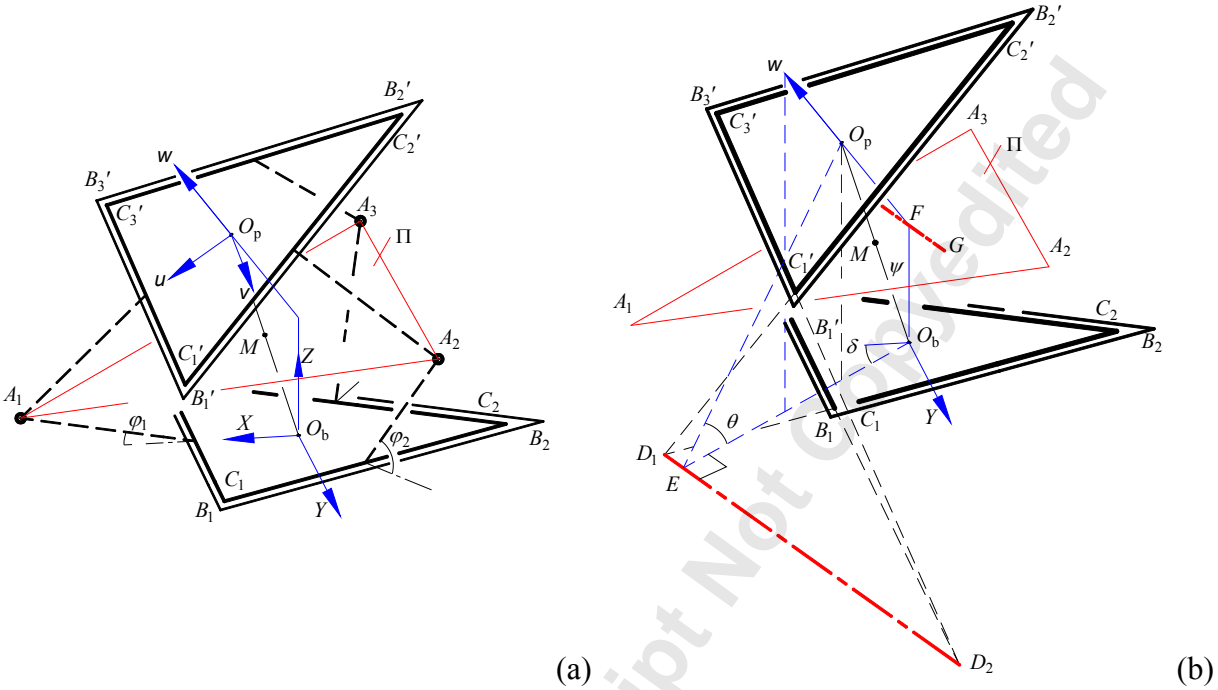

Fig 5. Kinematic model of the equivalent mechanism of the origami parallel structure

Journal of Mechanisms and Robotics. Received July 01, 2015;
Accepted manuscript posted October 16, 2015. doi:10.1115/1.4031808

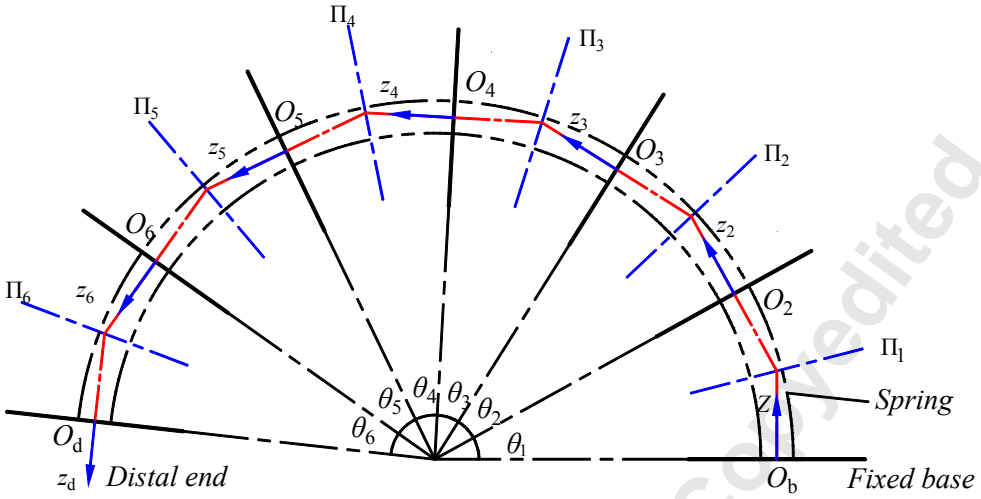

Fig. 6. Schematic kinematic model of the continuum robot with six modules

Journal of Mechanisms and Robotics. Received July 01, 2015;
Accepted manuscript posted October 16, 2015. doi:10.1115/1.4031808

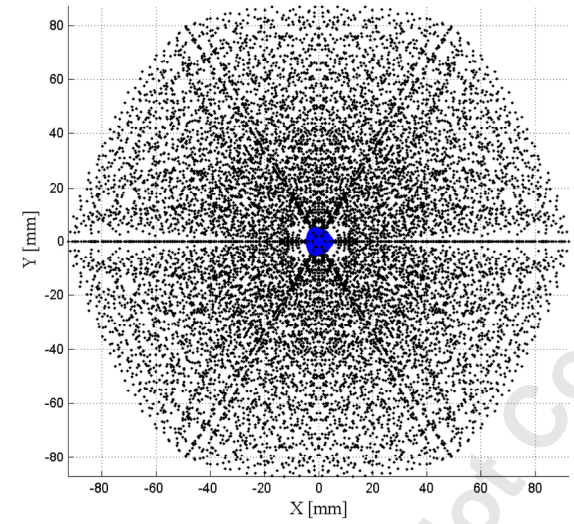

(a)

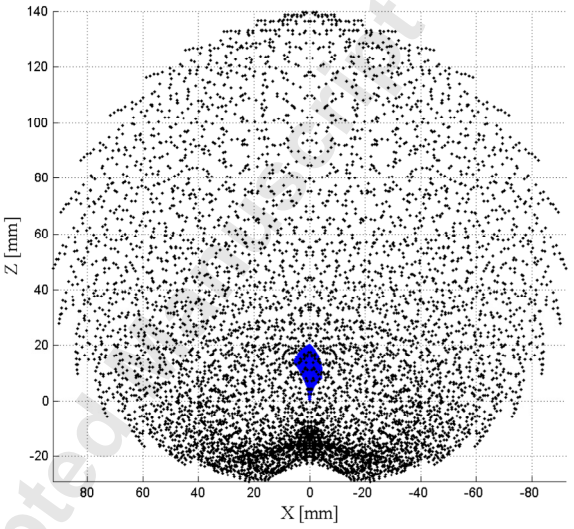

(b)

Fig. 7. Workspace of the continuum robot (a) view along Z-axis (b) view along Y-axis

Journal of Mechanisms and Robotics. Received July 01, 2015;
Accepted manuscript posted October 16, 2015. doi:10.1115/1.4031808

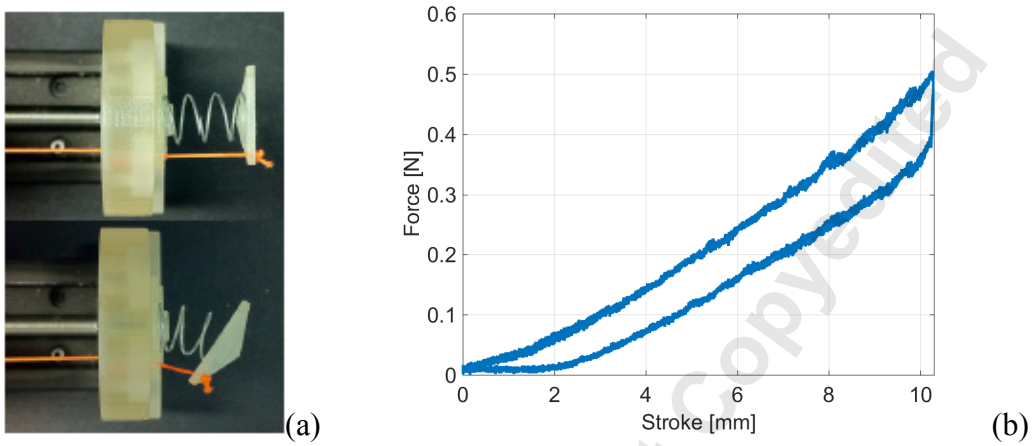

Fig. 8. Verification of the nonlinear performance of the compression spring (a) test set-up (b) bending performance of the compression spring

Journal of Mechanisms and Robotics. Received July 01, 2015;
Accepted manuscript posted October 16, 2015. doi:10.1115/1.4031808

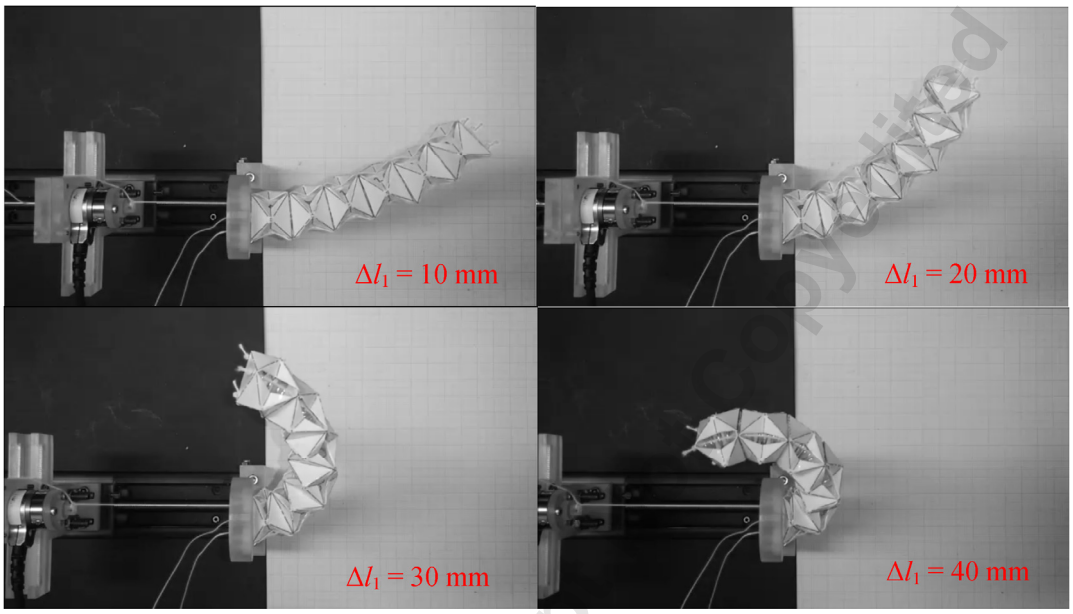

Fig. 9. Sequential stop figures of bending motion generated by one tensile force

Journal of Mechanisms and Robotics. Received July 01, 2015;
Accepted manuscript posted October 16, 2015. doi:10.1115/1.4031808

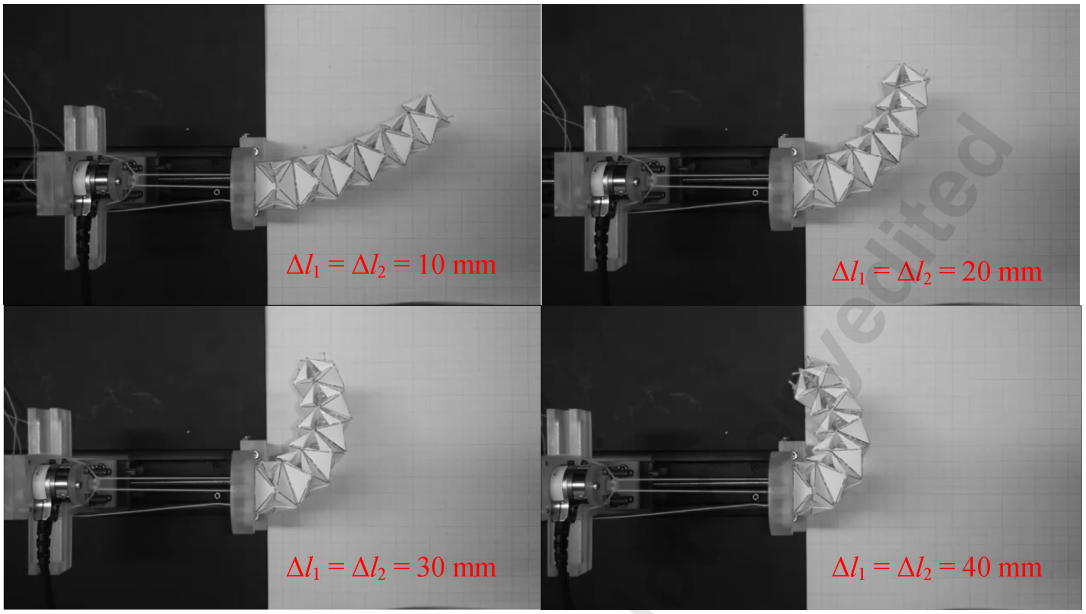

Fig. 10. Sequential stop figures of bending motion generated by two tensile forces

Journal of Mechanisms and Robotics. Received July 01, 2015;
Accepted manuscript posted October 16, 2015. doi:10.1115/1.4031808

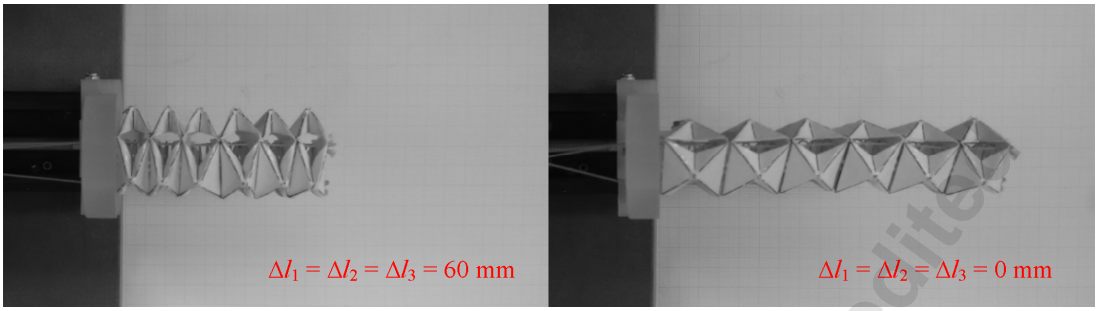

Fig. 11. The compact and elongated configurations of the extensible continuum robot